Cell Tissue Res (2017) 368:513–529
DOI 10.1007/s00441-017-2586-z

REGULAR ARTICLE

Midgut morphological changes and autophagy during metamorphosis in sand flies

Juliana Malta[1] · Matthew Heerman[2] · Ju Lin Weng[2] · Kenner M. Fernandes[1,3] · Gustavo Ferreira Martins[1] · Marcelo Ramalho-Ortigão[2,3,4]

Received: 27 October 2016 / Accepted: 6 February 2017 / Published online: 11 March 2017

Abstract During metamorphosis, holometabolous insects undergo significant remodeling of their midgut and become able to cope with changes in dietary requirements between larval and adult stages. At this stage, insects must be able to manage and recycle available food resources in order to develop fully into adults, especially when no nutrients are acquired from the environment. Autophagy has been previously suggested to play a crucial role during metamorphosis of the mosquito. Here, we investigate the overall morphological changes of the midgut of the sand fly during metamorphosis and assess the expression profiles of the autophagy-related genes *ATG1*, *ATG6*, and *ATG8*, which are associated with various steps of the autophagic process. Morphological changes in the midgut start during the fourth larval instar, with epithelial degeneration followed by remodeling via the differentiation of regenerative cells in pre-pupal and pupal stages. The changes in the midgut epithelium are paired with the up-regulation of *ATG1*, *ATG6* and *ATG8* during the larva-adult transition. *Vein*, a putative epidermal growth factor involved in regulating epithelial midgut regeneration, is also up-regulated. Autophagy has further been confirmed in sand flies via the presence of autophagosomes residing within the cytoplasmic compartment of the pupal stages. An understanding of the underlying mechanisms of this process should aid the future management of this neglected tropical vector.

Keywords Metamorphosis · Autophagy · Midgut development · Ecdysone · Sand flies

Gustavo Ferreira Martins and Marcelo Ramalho-Ortigão contributed equally to this work.

Electronic supplementary material The online version of this article (doi:10.1007/s00441-017-2586-z) contains supplementary material, which is available to authorized users.

✉ Marcelo Ramalho-Ortigão
mrortigao@gmail.com

[1] Departamento de Biologia Geral, Universidade Federal de Viçosa (DBG/UFV), Campus Universitário, Viçosa, Minas Gerais CEP 36570-900, Brazil

[2] Department of Entomology, Kansas State University (KSU), Manhattan KS 66506, USA

[3] Departamento de Entomologia, Universidade Federal de Viçosa (DBG/UFV), Campus Universitário, Viçosa, Minas Gerais CEP 36570-900, Brazil

[4] Present address: Department of Preventive Medicine and Biostatistics, Uniformed Services University of the Health Sciences (USUHS), Bethesda MD 20814, USA

Introduction

During metamorphosis, insects must be able to manage and recycle existing tissues, organelles and nutrients to develop fully into adults, as they are unable to acquire further food from the environment. In addition, for holometabolous insects, midgut remodeling is crucial for the digestive system to cope with the distinct feeding habits that may vary significantly between the larva and adult. The midgut remodeling process is coordinated by the proliferation and differentiation of stem cells into differentiated midgut cells, including digestive and endocrine cells (Wigglesworth 1972; for a review, see Hakim et al. 2010), and this is intensified during the larva to pupa transition. Midgut transformation involves the replacement of most larval midgut cells by new differentiated cells. In this transition during the life cycle, larval epithelial cells degenerate and, at the same time, are replaced by the differentiation and reorganization of regenerative cells present in the larval midgut (Neves et al. 2003a, b; Martins et al. 2006).

Autophagy has been previously suggested to play a crucial role during the metamorphosis of holometabolous insects and has been shown to serve as the principal mode of programmed cell death for the remodeling of larval tissues in favor of adult variants (Berry and Baehrecke 2007; McPhee et al. 2013; Rusten et al. 2004; Tian et al. 2013; Denton et al. 2009, 2012; Franzetti et al. 2012). Details associated with midgut remodeling during metamorphosis have been characterized in some blood-sucking dipterans including the major mosquito vectors *Aedes aegypti* and *Culex quinquefasciatus* (Nishiura et al. 2003; Okuda et al. 2007; Parthasarathy and Palli 2007; Ray et al. 2009; Fernandes et al. 2014, 2016). Recently, autophagy has been demonstrated to be under the direct influence of ecdysone signaling during development (Liu et al. 2015). Specifically, elements of the promoter for the autophagy-related gene *ATG1* in the silk worm *Bombix mori* allow *ATG1* to act as a primary response gene to the growth hormone and E93 transcription factor (Siegmund and Lehmann 2002). Moreover, the epidermal growth factor (EGF) Vein, which is associated with regulating epithelial midgut regeneration during infection in *Drosophila melanogaster* (Buchon et al. 2010), is also likely to be involved in the development of intestinal progenitor cells during the formation of the adult epithelium (Jiang and Edgar 2009; Biteau and Jasper 2011).

Phlebotomine sand flies (Diptera:Psychodidade) are known for their major role in the transmission of leishmaniasis, a neglected tropical disease caused by parasites of the genus *Leishmania*. As a holometabolous insect, sand flies develop, after egg hatching, via four larval stages followed by the pupal stage and finally into the winged adult (for reviews, see Killick-Kendrick 1999; Rangel and Lainson 2003; Lainson and Rangel 2005). During the transition from the immature stages to the adult, sand flies change their feeding habits from being detritivorous to being phytophagous and/or hematophagous (Sherlock 2003). Only females are hematophagous and such a feeding habit renders the sand fly female of epidemiological relevance.

The digestive tract in the larvae of sand flies has a relatively smooth tubular shape along its length (do Vale et al. 2007; Heerman et al. 2015), whereas in the adult, the abdominal midgut is more dilated and able to expand after food intake, including blood (Andrade-Coêlho et al. 2001; Sádlová and Volf 2009; Malta et al. 2016). In spite of several studies focused on the morphology of the midgut in both adults and larvae in sand flies (Gemetchu 1974; Rudin and Hecker 1982; Andrade-Coêlho et al. 2001; Secundino et al. 2005; Malta et al. 2016), studies pertaining to midgut remodeling or epithelial regeneration during metamorphosis and to the regulation of genes associated with autophagy are either scarce or non-existent.

The midgut plays crucial physiological roles in sand flies, including food intake, digestion and nutrient absorption and for the establishment of pathogens. Despite these vital roles, the morphophysiological processes that lead to the final shape of the midgut in adults are poorly understood. Our aim in this study is to combine details of the morphological (gross and detailed) changes undergone by the sand fly midgut during metamorphosis with the expression of the autophagy-related genes *ATG1*, *ATG6* and *ATG8* and of the putative sand fly EGF gene *Vein*. Our results reveal new insights into the biology of two sand fly species, namely *Lutzomyia longipalpis* and *Phlebotomus papatasi*, major vectors of *Leishmania infantum* and *Leishmania major*, respectively, providing important details of the midgut remodeling process that occurs during metamorphosis in sand flies.

Materials and methods

Sand flies

The two sand fly species used in our studies, *L. longipalpis* Jacobina strain (*LLJB*) and *P. papatasi* Israeli strain (*PPIS*) were reared in the Department of Entomology, Kansas State University, USA. Larvae were maintained in "larval pots", i.e., 250 or 500 ml plastic jars (Nalgene, Thermo Fisher Scientific) with an approximately 2-cm-thick bed made of dental plaster (Schein) and were fed on larval chow (a mixture of 50 % rabbit droppings and 50 % rabbit food). All larval stages and adult emergence were monitored daily. The various larval stages from larval stage 3 (L3) to pupae were separated according to stage and maintained in larval pots. Adults were routinely released into plexyglass rearing cages (15 × 15 × 15 cm or 25 × 25 × 25 cm).

We studied the following developmental stages of the sand fly: 3-day-old fourth instar larvae (or L4-3), the last stage of which still feeds and wanders and whose midgut is typically full of food and still contains the type II peritrophic matrix (PM2); 5-day-old fourth instar larvae (or L4-5), representing the last larval stage, which has stopped feeding and whose midgut is empty, with PM2 no longer being detectable; prepupae, during which the transition from the larval to pupal stages occurs; pupa 24 h (P24) and 72 h (P72), as representative time-points of early and late pupal stages; and newly emerged females, representing the adult stage. All recently emerged (RE) adult females used in the experiments below were less than 12 h old, as pupae were monitored until the night before emergence, and adults were released and collected for dissection the next morning. All adults were unfed (i.e., no water or sugar were offered).

Midgut morphology and ultrastructure during sand fly development

In the sand fly, the midgut and cell morphology during larval development and throughout metamorphosis was assessed by using the microscopic techniques outlined below.

Dissection

For histological analysis and transmission electron microscopy (TEM), five midguts of each developmental stage of *L. longipalpis* and *P. papatasi* were dissected in 0.1 M PBS (phosphate-buffered saline), fixed in 2.5 % glutaraldehyde solution (0.1 M sodium cacodylate buffer, pH 7.4) for at least 2 h, and kept at 4 °C in 0.1 M PBS until use. For immunofluorescence analysis, the midguts were dissected, fixed in Zamboni solution (2 % paraformaldehyde containing 15 % picric acid in 0.1 M sodium phosphate buffer) for 2 h and kept at 4 °C.

Histology

The fixed samples were washed in 0.1 M PBS, dehydrated in an ascending ethanol series (30-100 %), infiltrated in ethanol/historesin Leica (Biosystems Leica, Nussloch, Germany; 1:1) for 10 min, and embedded in historesin with hardener. Blocks were sectioned (3-μm-thick sections) and stained with hematoxylin and eosin (HE) or HE and toluidine blue (TB). Slides were mounted with Eukitt mounting medium (Sigma-Aldrich, St. Louis, USA), analyzed and photographed under an optical microscope Olympus BX 53 equipped with a digital camera (Olympus DP 73).

Transmission electron microscopy

Fixed samples (see Dissection) were post-fixed in 1 % osmium tetroxide in 0.1 M sodium cacodylate buffer for 2 h, protected from light. They were then washed three times in PBS, dehydrated in an ascending ethanol series (30-100 %) and pre-infiltrated in LRWhite resin solution (London Resin Company, UK) and 100 % ethanol (2:1) for 1 h, followed by another pre-infiltration of the same mixture at a ratio of 1:1 for 2 h. Subsequently, the samples were kept in pure resin for 24 h at 4 °C, and polymerization was carried out at 60 °C for 24 h in gelatin capsules. Ultrathin sections were contrasted with uranyl acetate solution (2 %) and lead citrate (0.2 %) and analyzed in a Zeiss EM 109 transmission electron microscope.

RNA extraction, reverse transcription, and real-time polymerase chain reaction

For reverse transcription with quantitative polymerase chain reaction (RT-qPCR), whole-body RNA of *L. longipalpis* L3, wandering L4, pupae, or adult females was isolated by using TRIzol (Invitrogen-Thermo Fischer, Carlsbad, Calif., USA) and for each group of insects, RNA isolation was conducted in triplicate. RNA quality was assessed by electrophoresis on 1 % agarose-5 % formaldehyde in 1× MOPS gel prior to first-strand cDNA synthesis by using the Superscript III reverse transcription kit (Invitrogen-Thermo Fischer) as described (Coutinho-Abreu et al. 2010). mRNA levels for the various developmental stages were quantified with iQ SYBER Green Supermix (Bio-Rad, Hercules, Calif., USA) at 95 °C for 5 min followed by 40 cycles of 95 °C for 30 s, 57 °C for 30 s and 72 °C for 45 s in a Realplex^4 Master cycler (Eppendorf, Hauppauge, N.Y., USA). Fold changes were measured via the ΔΔCt method and calibration against the expression of each L3 transcript was used for comparison (Schmittgen and Livak 2008). Sequences for *ATG1* (accession no. LLOJ007855), *ATG6* (accession no. LLOJ007047), *ATG8* (accession no. LLOJ007649) and *Vein* (accession no. LLOJ001534) were obtained from homology to *D. melanogaster* sequences and by using Blastn and/or Blastp against *L. longipalpis* sequences available in the VectorBase (https://www.vectorbase.org/blast). The results of these queries are summarized in Supplemental Table 1. Primer sequences were generated by using Primer3 (http://biotools.umassmed.edu/bioapps/primer3_www.cgi). Primers for *Vein* were based on the sequences used in our previous study (Heerman et al. 2015). The polymerase chain reaction (PCR) amplicon sequence was assessed by direct sequencing (data not shown). All Blastp data and primer sequences used in this study are summarized in Supplemental Table 1 and Supplemental Table 2.

Immunofluorescence: markers of apoptosis, autophagy, and cell proliferation

Midguts (n = 3 per developmental stage) previously fixed in Zamboni fixative were washed three times in 0.1 M PBS/1 % Triton X-100 (PBST) and incubated separately with either anti-caspase-3 (Sigma-Aldrich, St. Louis, Mo., USA; 1:1000), anti-nuclear protein phosphohistone H3 (PH3; 1:1000), or anti-LC3A/B (1:100; Cell Signaling Technology, Beverly, Mass., USA) for 24 h at 4 °C in PBST. The LC3A/B antibody is the mammalian version of anti-ATG8. Samples were washed again, then incubated with secondary anti-rabbit antibody conjugated to fluorescein isothiocyanate (FITC; Sigma-Aldrich) in PBS for 24 h at 4 °C (1:500), washed three times in PBS (10 min each), mounted with Moiwol solution (whole-mount) and subsequently analyzed and photographed under a confocal microscope (Zeiss LSM 510; Carl Zeiss Microscopy, Thornwood, N.Y., USA). For PH3, samples were also analyzed under an epifluorescence microscope (Olympus BX60 equipped with a digital camera).

For labeling with rabbit anti-*D. melanogaster* ATG6 (Beclin1) polyclonal antibody, samples of sand fly midgut were washed four times for 30 min each with PBS containing 0.3 % Triton X-100 (PBST) and then blocked with PBS containing 1 % bovine serum albumin (BSA) for 30 min at room temperature. Antibodies were diluted 1:500 in PBST immediately prior to use. Following primary antibody incubation overnight at 4 °C, samples were washed as indicated above and incubated overnight at 4 °C with Alexa-Fluor-594-conjugated goat anti-rabbit antibody

(Invitrogen-Thermo Fischer) diluted 1:1000 in PBST. After another round of washes (as above), the nuclei were stained for 5 minutes with 10 μg/ml 4,6-diamidino-2-phenylindole (DAPI; Invitrogen-Thermo Fischer). The specificity of fluorescence signals was evaluated in negative controls treated only with the second FITC-conjugated antibody (without the primary antibodies). Negative controls were mounted and analyzed as described above (see below).

Midgut morphometry

The height of the digestive cells was measured in digital micrographs of the histological sections. Five cells were measured in each individual ($n = 5$) of each stage/phase of development, and only cells with a striated border and apparent basal lamina were considered. The measurements were performed with the aid of the software Image-ProPlus Windows version 4.2 (Media Cybernetics, Rockville, Md., USA). The data were submitted to an analysis of variance (ANOVA) followed by Tukey's test ($P < 0.001$) to test the differences between the stages of the same species and to Student's *t*-test to detect differences between the same developmental stage among species ($P < 0.001$).

In addition to the measurements of midgut cells, we also determined the general dimensions of whole guts from *L. longipalpis*. Larval gut that had been previously imaged by using anti-ATG6 antibodies (see Immunofluorescence: markers of apoptosis, autophagy, and cell proliferation) was re-analyzed for length and width by using the Zeiss LSM 700 confocal microscope (Carl Zeiss Microscopy) and axial ratios (L/W) were calculated. The guts of five animals each from the three developmental stages, namely L3, wandering L4 and pupae, and of five adult females were placed into PBS and fixed for 20 min at room temperature with 4 % paraformaldehyde in PBS. Samples were mounted in FluorSave anti-photobleaching reagent (CalBiochem-EMD Millipore, Billerica, Mass., USA) and images were obtained via a Zeiss LSM 700 confocal microscope (Carl Zeiss Microscopy). In addition, images were manipulated and midgut length, width and axial ratios were measured by using the Zen confocal microscope software (Zeiss).

Sequence alignments, phylogeny and putative ecdysone-response element prediction

To determine putative ecdysone-response element regions upstream of *ATG1*, genomic sequence (AJWK01026160.1) was obtained from the European Nucleotide Archive (http://www.ebi.ac.uk/ENA/). This sequence was searched for the presence of canonical and non-canonical ecdysone-responsive sequence elements as described previously (Cherbas et al. 1991).

Results

Changes in midgut morphology and ultrastructure during sand fly development

Three-day-old L4 (L4-3) The midgut epithelium of L4-3 displayed similar morphologies in both *L. longipalpis* (*LLJB*) and *P. papatasi* (*PPIS*), with a single layer of columnar basal cells on top of a basal lamina and coated externally by a muscle layer (Fig. 1a, b). Digestive cells and stem cells were the principal cell types observed. The digestive cells had a brush border and a nucleus with predominantly decondensed chromatin and an evident nucleolus (Fig. 1a). Stem cells were small, were located at the basal region of the digestive cells, and were present either isolated as single cells or in small clusters (Fig. 1b). The midgut lumen was filled by the food bolus surrounded by PM2 (Fig. 1a, b, Supplementary Fig. 1a). The average height of the columnar cells was measured at 49.0 ± 2.1 μm in *LLJB* and 54.5 ± 3.9 μm in *PPIS* ($P > 0.001$) and was statistically different from heights at other stages ($P < 0.001$; Supplementary Fig. 2a).

Microvilli were developed and well organized in parallel, and numerous mitochondria were seen at the apex of the digestive cells. The median region of the cytoplasm of the cells contained vacuoles, especially in *PPIS* (Fig. 1d, e). Adjacent cells were joined by septate junctions, present primarily in the apical portion (Fig. 1d, f). In the basal region of these cells, the plasma membrane had invaginations, forming a basal labyrinth associated with mitochondria (Fig. 1g). In addition to the basal lamina, internal and external muscle bundles surrounded the midgut epithelium (Fig. 1c).

Stem cells were present throughout the midgut of the two sand fly species and, as indicated previously, were visible either as single cells or forming small clusters with as many as three cells on the basal region of the epithelium. These cells had little cytoplasm and a central nucleus. The stem cells were poor in organelles, possessing few mitochondria and rough endoplasmic reticulum (rer). The nucleus of the stem cells was predominantly composed of decondensed chromatin, and their plasma membrane displayed few invaginations (Figs. 1b, g, Supplementary Fig. 1b).

In *PPIS*, "bubble-like" protrusions or blebs were observed on the apical portion of epithelial cells (Fig. 1d, Supplementary Fig. 1a) and were suggestive of the apocrine secretion that follows the rupture of blebs and the release of the apical cytoplasm and organelles into the lumen. Our results suggest that the degeneration of the epithelium during the larval development in *PPIS* starts at this stage (L4-3), with the degeneration of the digestive cells. In contrast, in *LLJB*, such morphological features were absent at this stage and unlike *LLJB*, the cytoplasm of degenerating digestive cells in *PPIS* was highly vacuolated (Fig. 1d–f) and remnants of digestive cells could also be observed (Fig. 1e).

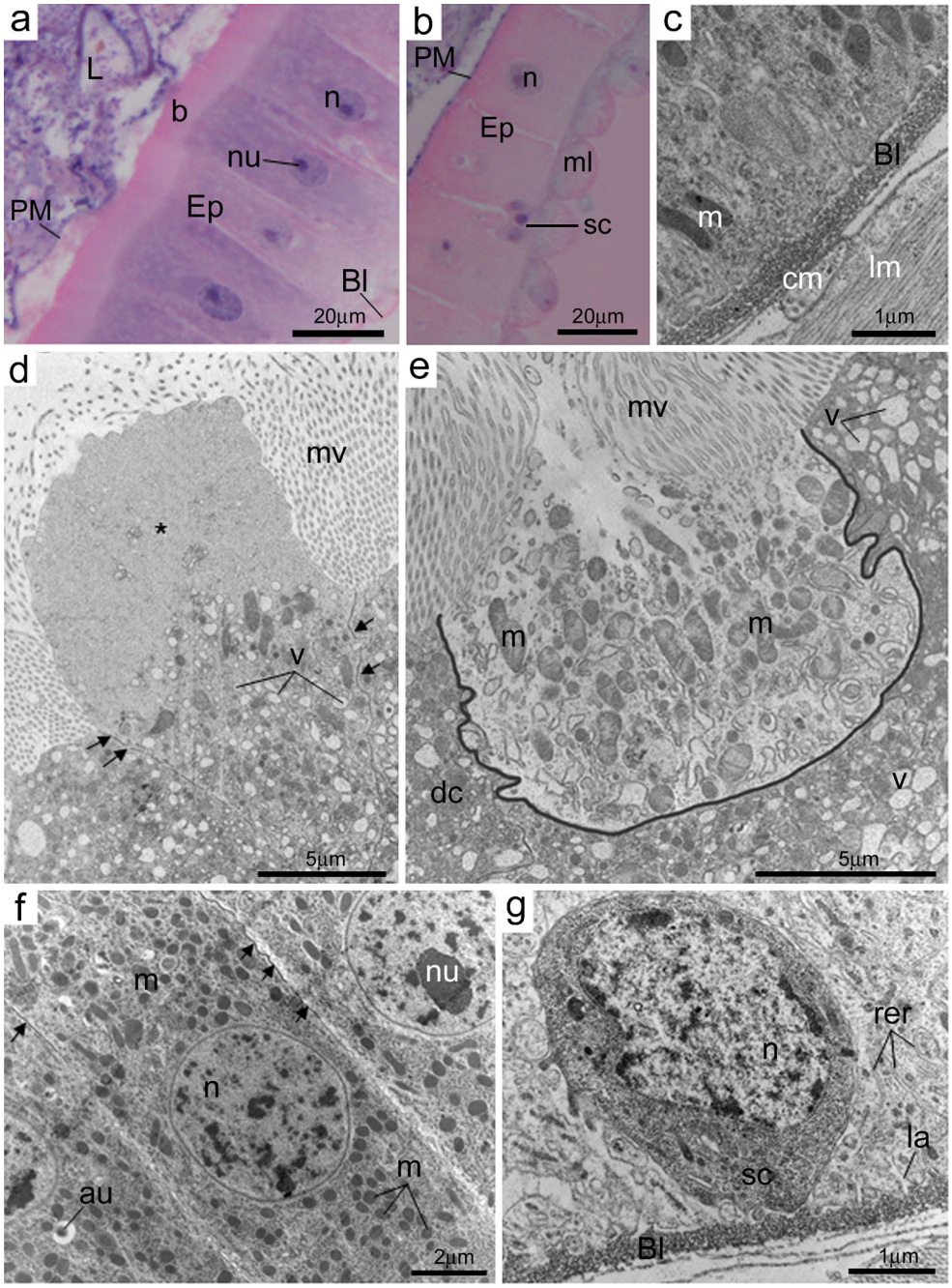

Fig. 1 Cellular organization of midguts from larvae of *Lutzomyia longipalpis* Jacobina strain (*LLJB*) and *Phlebotomus papatasi* Israeli strain (*PPIS*). Histological sections (**a**, **b**) stained with hematoxylin and eosin (HE) and transmission electron micrsosocpy (TEM, **c-g**) of the midgut of 3-day-old fourth instar larvae of *LLJB* (**a–e**) and *PPIS* (**f**,**g**). **a** Epithelium (*Ep*) consisting in columnar digestive cells with central nuclei (*n*) and developed brush border (*b*). The midgut lumen (*L*) is filled with the food bolus surrounded by a peritrophic matrix (*PM*). *Bl* Basal lamina, *nu* nucleolus. **b** Midgut epithelium (*Ep*) with columnar digestive cells with their central nucleus (*n*) and stem cells (*sc*) on the basal region of the epithelium (*ml* muscle layer). **c** Basal region of a digestive cell lying close to the basal lamina (*Bl*) and associated with mitochondria (*m*). *cm* Circular muscle, *lm* longitudinal muscle. **d** Apical portion (*asterisk*) of a digestive cell being ejected toward the midgut lumen. The cytoplasm contains many vacuoles (*v*). The median apical portion of the cell adheres to the adjacent cells by septate junctions (*arrows*). *mv* Microvilli. **e** Apical region and microvilli (*mv*) of digestive cells (*dc*) and a remnant of a digestive cell (*outlined in black*). *m* Mitochondria, *v* vacuoles of various sizes. **f** Perinuclear portion of three digestive cells containing a nucleus (*n*) with decondensed chromatin and a nucleolus (*nu*), mitochondria (*m*), and autophagic vacuoles (*au*). The cells are joined by septate junctions (*arrows*) at their apical portion. **g** Stem cell (*sc*) in the basal region of the midgut epithelium. The nucleus (*n*) of the cell occupies most of its cytoplasm, which has few organelles. Close to the basal lamina (*Bl*), invaginations of the plasma membrane of the digestive cell are seen forming the basal labyrinth (*la*). *rer* Rough endoplasmic reticulum

Five-day-old L4 (L4-5) During this stage, the morphology of the midgut epithelium was similar in both *LLJB* and *PPIS*, with columnar cells being slightly shorter than those observed in L4-3 (Fig. 2a and c). The assessed height of the digestive cells in L4-5 larvae was shorter than the height observed for the same cells in L4-3 larvae ($P < 0.001$) in both *LLJB* (assessed cell height of 27.9 ± 1.36 μm) and *PPIS* (assessed height of 34.0 ± 2.24 μm; Supplementary Fig. 2a). Unlike L4-3, the PM was not visible during the L4-5 stage (Fig. 2a, Supplementary Fig. 3a) and the degenerative process of the midgut cells was underway in the two sand fly species investigated. Here, the degenerative process was marked by the presence of cytoplasmic vacuoles within the digestive cells in both flies (Fig. 2b, Supplementary Fig. 3b) and by cytoplasmic protrusions or blebs (not shown) similar to those present in the L4-3 stage in *PPIS*.

Pre-pupa In pre-pupa, the degeneration process continued with the release of portions of the cytoplasm of the larval midgut epithelium, simultaneously with the growth of the new epithelium (Fig. 2d-g). In *LLJB*, individualized stem cells were observed on the basal portion of the epithelium, whereas the cells undergoing differentiation (presumably digestive cells) formed a single layer (Supplementary Fig. 3c). In contrast, the *PPIS* midgut lumen was completely filled, probably by the remnants of the epithelium of the larva, ejected during the process of larval epithelium degeneration (Fig. 2c). The average assessed height of the differentiating cells in pre-pupae was even smaller than in the larvae of *LLJB* (18.3 ± 0.8 μm) and *PPIS* (16.8 ± 0.62 μm; $P < 0.001$; Supplementary Fig. 2a).

As yet undetermined cells in an intermediate stage of differentiation grew toward the midgut lumen, forming a new epithelium with nuclei at various positions. These cells had short microvilli and nuclei with decondensed chromatin and an evident nucleolus (Fig. 2d, e). Stem cells were also seen in groups in *PPIS*; they had cytoplasm with few organelles and a central nucleus occupying almost all the cytoplasm. Multilamelar bodies and cytoplasmic vacuoles were present within the differentiating cells. Several of these vacuoles corresponded to autophagic vacuoles with organelle remains or debris lying inside them (Fig. 2f, g).

Pupa at 24 h (P24) The general characteristics of the midgut epithelium in P24 were similar for the two species. The growing adult epithelium had short cells (Fig. 3a-c, e), with an average height of 11.3 ± 0.5 μm in *LLJB* and 13.7 ± 0.92 μm *PPIS* ($P < 0.001$; Supplementary Fig. 2a).

In both species, the lumen was filled with homogeneous and electron-dense material, probably resulting from the histolysis of the larval epithelium (Fig. 3a-c, e). In differentiating cells in *LLJB*, mitochondria were seen mainly in the apical region or just above the nucleus, and short microvilli that were sometimes folded were also observed (Figs. 3d,d 4b). The rer was well developed (Fig. 3f) and multilamellar bodies were present in the cytoplasm of differentiating cells (Fig. 3g).

Fig. 2 Cellular organization of midguts from larvae and pre-pupae of *LLJB* and *PPIS*. Histological sections (**a**, **c**) and TEM (**b**, **d**–**g**). **a** Midgut epithelium (*Ep*) of *LLJB* 5-day-old fourth instar larvae, showing digestive cells with a central nucleus (*n*). *Arrows* Stem cells, *L* midgut lumen, *lm* longitudinal muscle. HE staining. **b** Numerous vacuoles (*v*) in the cytoplasm of digestive cells of *LLJB* L4-5 (*n* nucleus). **c** Midgut epithelium (*Ep*) of *PPIS* pre-pupa, with short and disorganized cells. The lumen (*L*) is filled with intensely colored material. HE + toluidine blue staining. **d** Differentiating cells of *LLJB* pre-pupa with prominent nucleus (*n*) and cytoplasm with few organelles and microvilli (*mv*). *Ld* Lipid droplets, *nu* nucleolus, *rer* rough endoplasmic reticulum. **e** Differentiating cell in *PPIS* with few microvilli (*mv*). *n* Nucleus with decondensed chromatin, *BL* basal lamina. **f** Electron-lucent stem cells (*sc*) of prepupae of *PPIS*. Their cytoplasm is poor in organelles and their nuclei (*n*) occupy a large part of the cell (*au* autophagic vacuoles, *dc* differentiating cell, *Bl* basal lamina). **g** Portion of the cytoplasm of a cell in degeneration in *PPIS* prepupa. Autophagic vacuoles (*au*) with organelle debris (*arrows*) are visible in the cytoplasm of cells undergoing autophagy. Multilamellar bodies (*ml*), hallmark of autophagy, are also observed (*inset*)

Pupa at 72 h (P72) The morphology of the midgut epithelium at this stage was similar to that observed in P24, with short cells having an average height of 14.4 ± 0.75 μm in *LLJB* and 17.4 ± 0.7 μm in *PPIS* ($P < 0.001$; Supplementary Fig. 2a). Folds in the epithelium appeared in both species as the newly formed epithelium increased in size (Figs. 4a, Supplementary Fig. 3d). Similar to the previous stage, the lumen of the midgut was filled by electron-dense material (Fig. 4b, c). Stem cells were found at the base of the epithelium (Fig. 4d). As noted above for P24, differentiating cells in P72 also grew toward the lumen and mitochondria were also present in the apical region (Fig. 4b).

RE adults The epithelium of the midgut in RE adults was similar in both species. It consisted in tall cells with an assessed height of 30.1 ± 1.09 μm in *LLJB* and 26.36 ± 0.69 μm in *PPIS* ($P < 0.001$; Supplementary Fig. 2a). The apical region of the digestive cells of both species showed short microvilli arranged in parallel. The epithelial cells had a nucleus in the center of the cell with predominantly decondensed chromatin and an evident nucleolus (Fig. 4e, f, Supplementary Fig. 3e, f). The digestive cells also displayed invaginations of the plasma membrane, forming a discrete basal labyrinth in the basal region (not shown). The cytoplasm of these cells contained few organelles, including mitochondria and an undeveloped rer. Adjacent digestive cells were joined by smooth septate junctions (Fig. 4e). The material in the lumen from the degeneration of the remaining larval epithelium was almost absent, and no stem cells were seen at this stage (Fig. 4f).

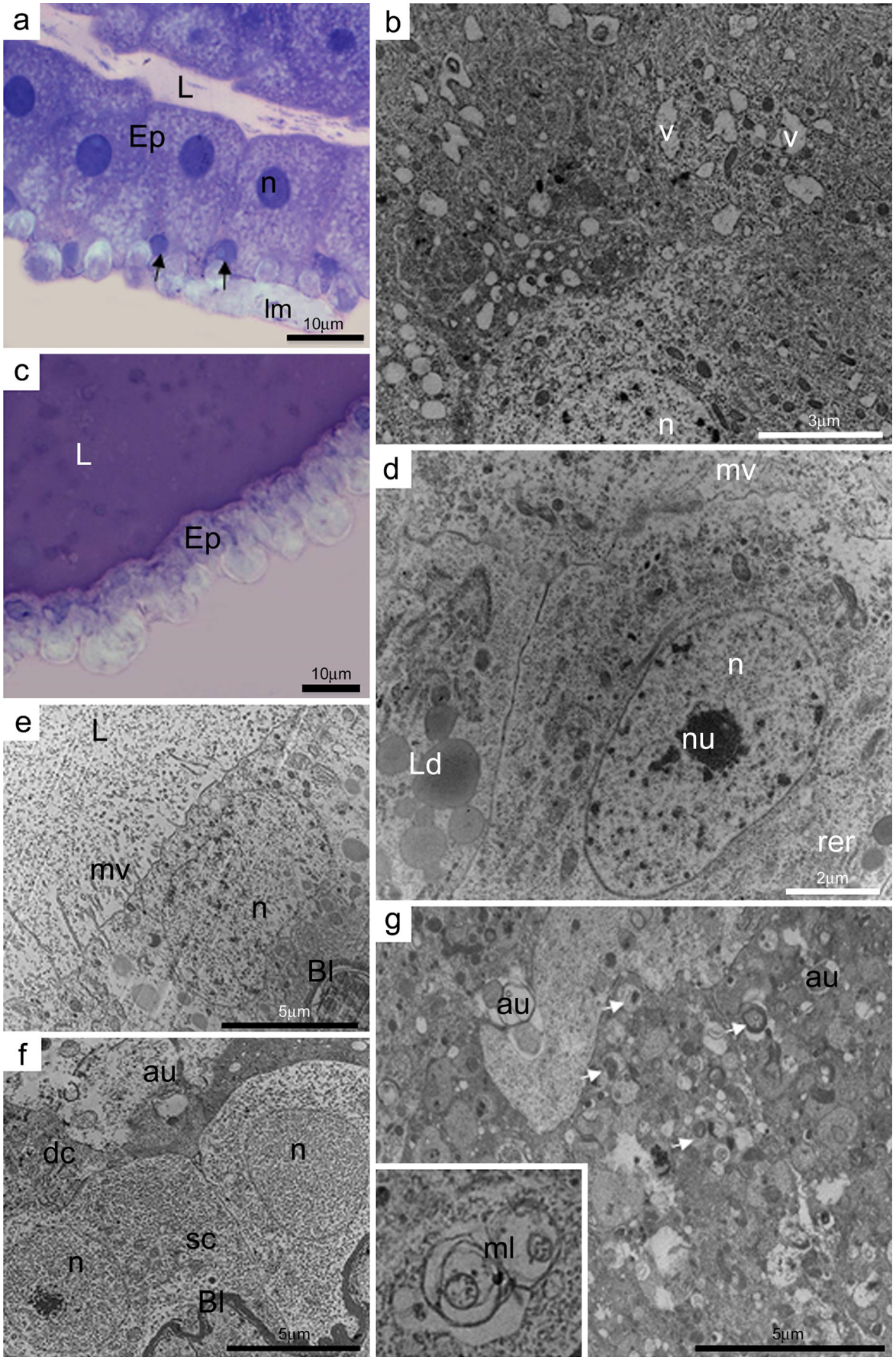
a
L
Ep
n
lm
10μm
b
v
v
n
3μm
c
L
Ep
10μm
d
mv
n
nu
Ld
rer
2μm
e
L
mv
n
Bl
5μm
f
au
dc
n
sc
n
Bl
5μm
g
au
au
ml
5μm

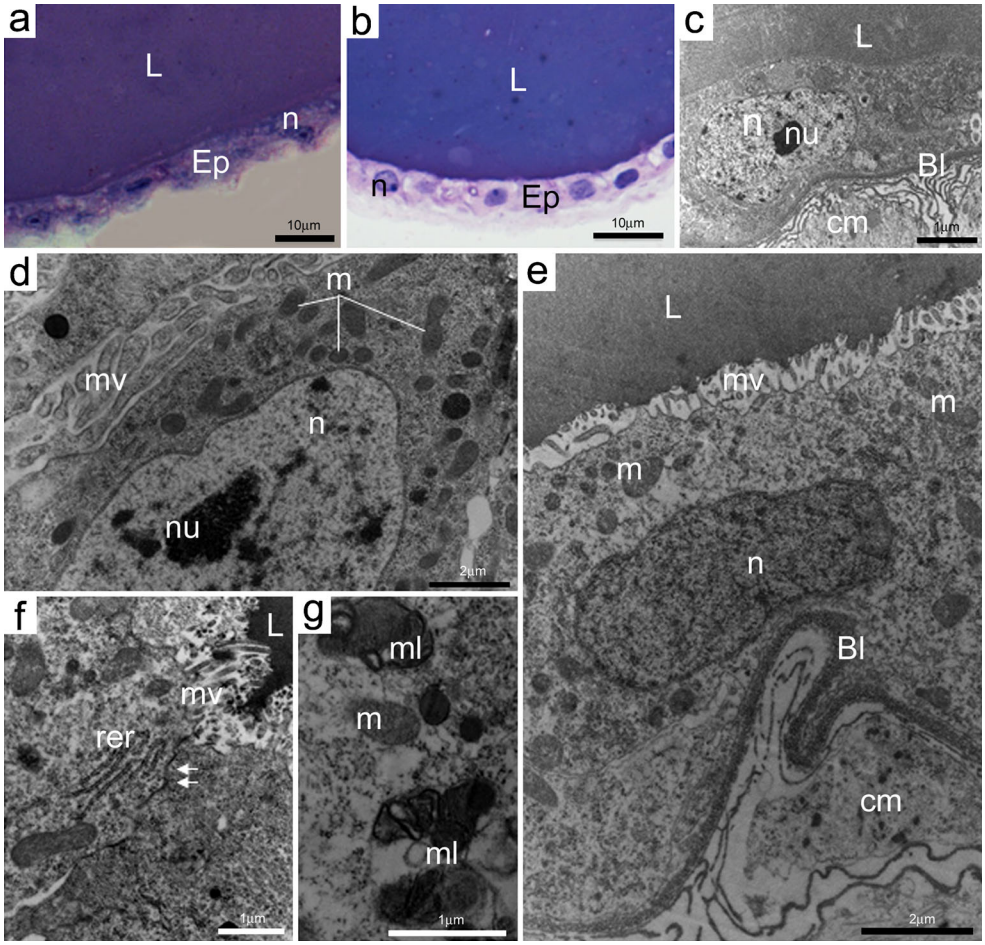

Fig. 3 Cellular organization in midguts from pupae of *LLJB* and *PPIS*. Histological sections (**a**, **b**) and TEM (**c**–**g**) of midguts from pupae 24 h after onset of pupation. **a**, **b** Midgut epithelium (*Ep*) with flattened cells in *LLJB* (**a**) and in *PPIS* (**b**). *L* Midgut lumen, *n* nucleus. HE + toluidine blue staining. **c** Differentiating cell in *LLJB* (*n* nucleus with decondensed chromatin, *nu* nucleolus). The midgut lumen (*L*) is filled with electron-dense material (*Bl* basal lamina, *cm* circular muscle). **d** Differentiating cell in *LLJB* with nucleus (*n*) having a predominance of decondensed chromatin and a nucleolus (*nu*). Microvilli (*mv*) are sparse and short (*m* mitochondria). **e** Differentiating cell in *PPIS* with a few short microvilli (*mv*). The midgut lumen (*L*) is filled with electron-dense material (*Bl* basal lamina, *cm* circular muscle layer, *m* mitochondria, *n* nucleus with decondensed chromatin). **f** Two adjacent digestive cells in *PPIS*. Short microvilli (*mv*) are seen in the apical region and a few mitochondria and developed rough endoplasmic reticulum (*rer*) are present in the cytoplasm. The cells are joined by septate junctions (*arrows*) at the apical portion (*L* lumen). **g** Detail of a cell undergoing differentiation in *PPIS*. Note the presence of multilamellar bodies (*ml*) and a few mitochondria (*m*)

In addition to the specific cellular changes outlined above, we were also interested in measuring the overall midgut dimensions and axial ratios (L/W) in all four major developmental stages (L3, L4, pupa and adult) as a means to identify developmental timing. Using confocal microscopy, we determined no significant difference in midgut length between L3, pupa and adult sand flies (Supplementary Fig. 2b). However, the L4 gut was significantly longer (roughly 200 μm) than the average midgut length in the pupa and in the adult sand fly. In addition to length, the average width of the L4 midgut was roughly 100 μm wider than any other stage observed (Supplementary Fig. 2c). This correlated with a significantly lower value for the axial ratio observed in L4 in comparison with pupae (Supplementary Fig. 2d). These observations provided us with a guide to the specific midgut morphologies as the insect approached, proceeded through and exited metamorphosis.

Expression profiles of ATG1, ATG6, ATG8 and Vein during *LLJB* development

Using RT-qPCR, we measured the transcript levels for the genes for the early autophagosome kinase (*ATG1*) and for the beclin-domain-containing protein (*ATG6*), for the sequestration gene (*ATG8*) and for the levels of the putative EGF *Vein*. We compared third instar (L3) larvae, wandering L4, newly formed pupae and adult flies by RT-qPCR. For *ATG1*, we observed an approximately 10-fold increase in transcript levels for tested pupae compared with all other developmental stages. A non-significant increase was observed for

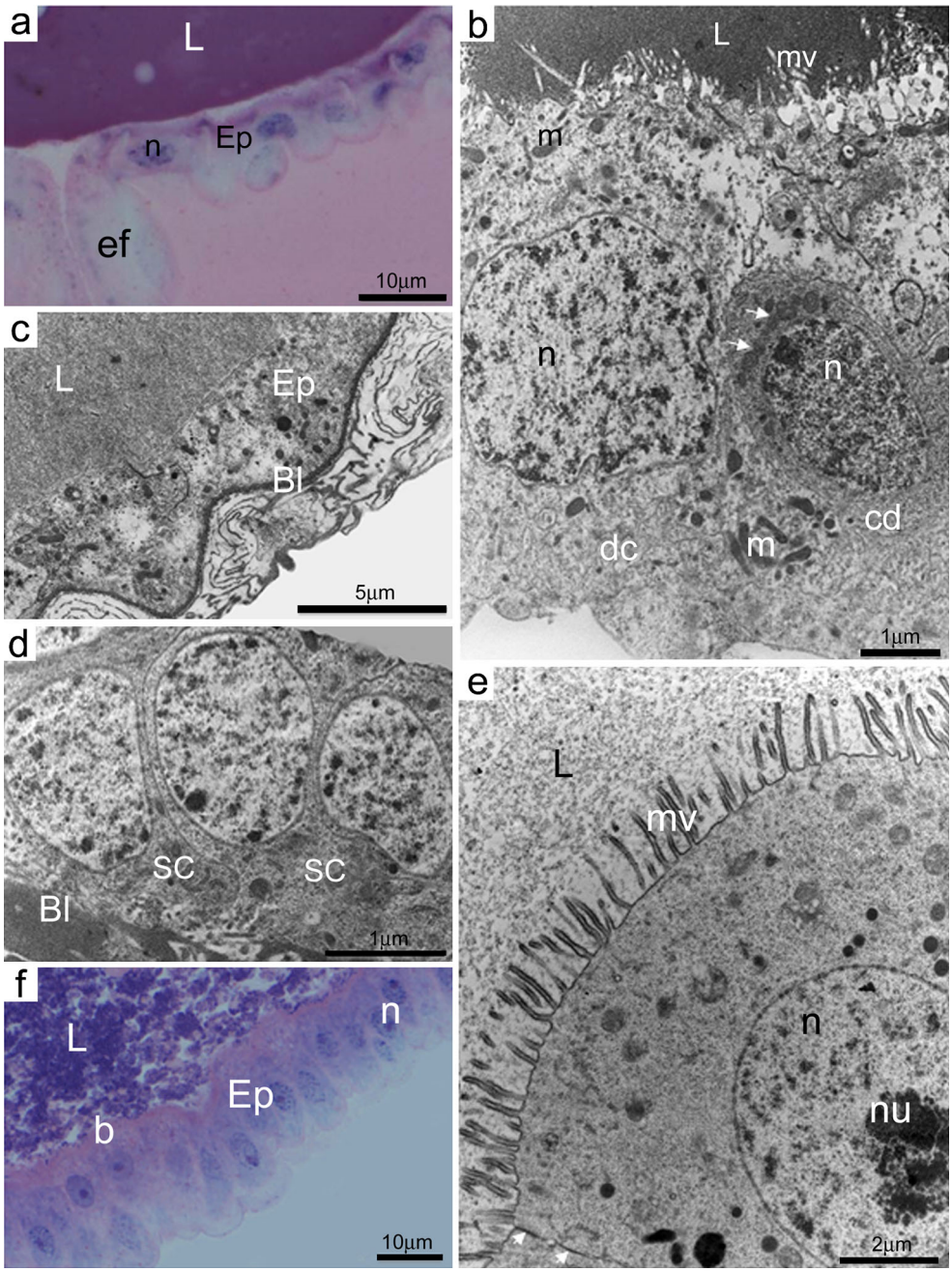

Fig. 4 Cellular organization in midguts from 72 h pupae and recently emerged (RE) adults of *LLJB* and *PPIS*. Histological sections stained with HE (**a**, **f**) and TEM (**b**–**e**) of the midgut of P72 (**a**–**d**) and RE adult females (**e**, **f**). **a** Midgut epithelium (*Ep*) of *PPIS* with flattened cells (*ef* epithelial fold, *L* strongly stained lumen, *n* nucleus). **b** Epithelium showing a pre-digestive cell (*dc*) and a cell in differentiation (*cd*) with accumulation of mitochondria (*arrows*) in the apical region in midgut in *PPIS* (*m* mitochondria in *dc*, *n* nucleus, *mv* short disorganized microvilli). **c** Epithelium (*Ep*) under reconstruction with flattened cells in midgut in *LLJB* (*L* electron-dense midgut lumen, *Bl* basal lamina). **d** Three stem cells (*SC*) in the basal region of *LLJB* midgut epithelium (*Bl* basal lamina). **e** Apical portion of a digestive cell with central nucleus (*n*) in midgut of *PPIS*. Note microvilli (*mv*) arranged in parallel at the apex. Adjacent cells are joined by septate junctions (*arrows*). *L* Electron-lucent lumen, *nu* nucleolus. **f** Midgut epithelium (*Ep*) of *PPIS* with columnar digestive cells having a central nucleus (*n*) and microvilli (*mv*). *L* Lumen

ATG6 in L4 larva, coupled with a significant >200-fold increase for the transcript for pupae compared with other stages (Fig. 5a). Peak increase for *ATG8* expression occurred at L4 and pupae vs. other stages. In the case of *Vein*, a 30-fold increase was observed for both L4 and pupa in comparison with L3 and adult ($P < 0.05$; Fig. 5b).

Markers for cell proliferation (mitosis), autophagy and apoptosis during sand fly development

A few cells positive for PH3 were observed in the midgut of the two sand fly species investigated. PH3-positive signals were clearly detected in larval stage L4-5 and in pupal stages P24 and P72 in both types of fly (Fig. 6). Although our analyses provided no quantitative data on the number of positive cells for PH3, a variation in the number of positive markers was detected between the developmental stages.

We also assessed the presence of pro-autophagic organelles and the expression of pro-apoptotic proteins in the midgut cells of sand fly during larval development, pupation and metamorphosis. To confirm the presence of autophagic vacuoles (autophagosomes) in the midgut of sand flies, we used the anti-LC3A/B (ATG8) antibody. Positivity for anti-LC3A/B was observed in pre-pupa, P24 and P72 in *LLJB* and in P24 and P72

in *PPIS* (Fig. 7). Immunofluorescence assays with the anti-caspase-3 antibody revealed that caspase activity was present in the pre-pupa and P72 stages of *LLJB*, whereas caspase-3 detection was observed in pre-pupa, P24 and P72 in *PPIS* (Fig. 7). A summary of the results obtained following immunofluorescense assays to determine the presence or absence of apoptosis and/or autophagy as a mechanism involved in the development and pupation in sand flies is shown in Table 1.

We further probed the sand fly midgut using polyclonal antibodies targeting ATG6. The anterior midgut region of pupae showed staining for ATG6 in the cytoplasm of epithelial cells (Fig. 8a) where autophagosomes were expected to be present (Fig. 8b). For the remaining stages investigated, namely L3, L4 and adult, the ATG6 antibody revealed little to no signal in the anterior midgut (Fig. 8b-e).

Linking ecdysone with autophagy

We previously mentioned that growing evidence supports the idea that ecdysone hormone action is directly linked to autophagy through the promoter of response genes, specifically *ATG1*. At least for *LLJB*, we identified a putative promoter for *ATG1*. Three putative ecdysone responsive element half-sites that have been described by Cherbas et al. (1991) and that may react to ecdysone signaling (Fig. 9) were also identified in the *ATG1* sequence of *LLJB* (*LlATG1*). Additionally, the *LlATG1*

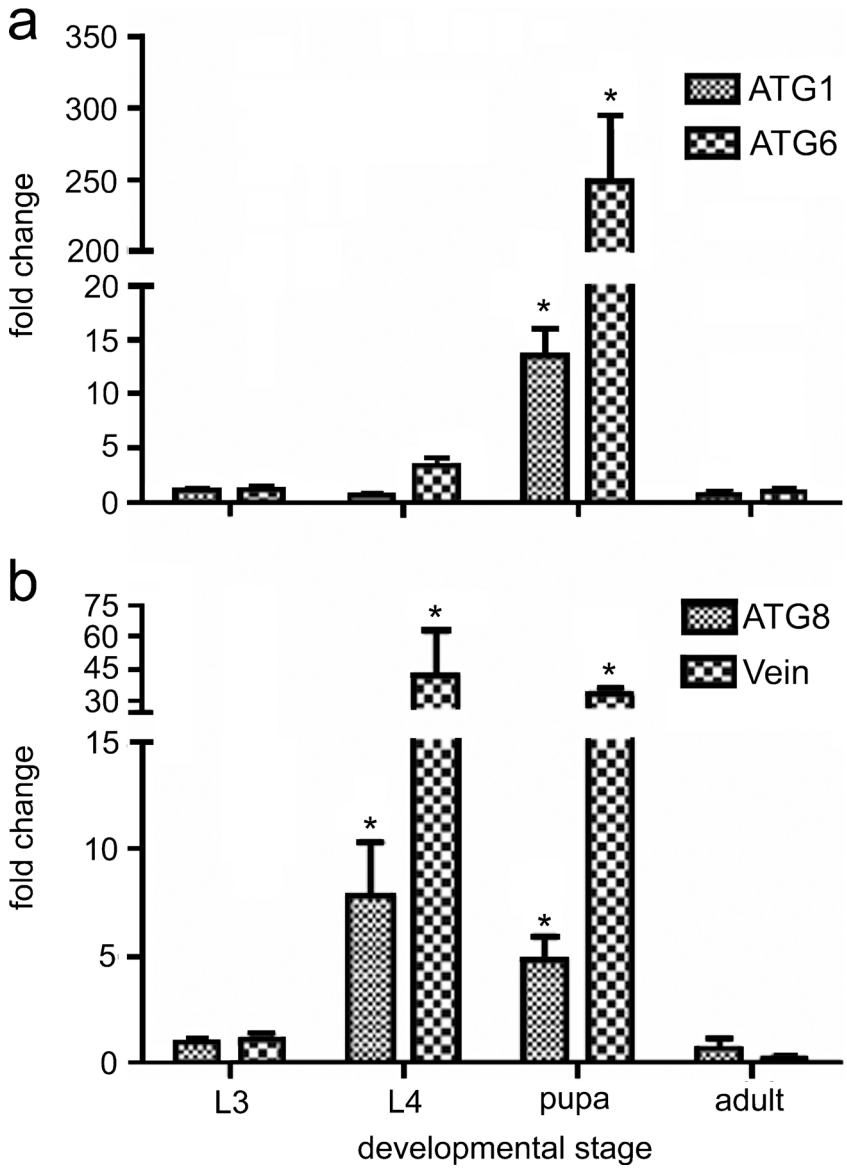

Fig. 5 mRNA expression profiles of autophagy-related genes *ATG1*, *ATG6* and *ATG8* and the epithelial regeneration *Vein* gene in *LLJB*. RNA was extracted from the midguts of feeding larvae (*L3*), non-feeding larvae (*L4*), early pupae (*pupa*) and adult sand flies (*adult*). After first-strand cDNA synthesis, DNA was amplified by using gene-specific primers. **a** Fold change and standard errors for the transcripts encoding *ATG1* and *ATG6*. **b** Fold measurements and errors for *ATG8* and *Vein* transcripts. A one way analysis of variance (ANOVA) was performed with a Tukey post test for multiple comparisons to measure statistical significance ($P < 0.05$)

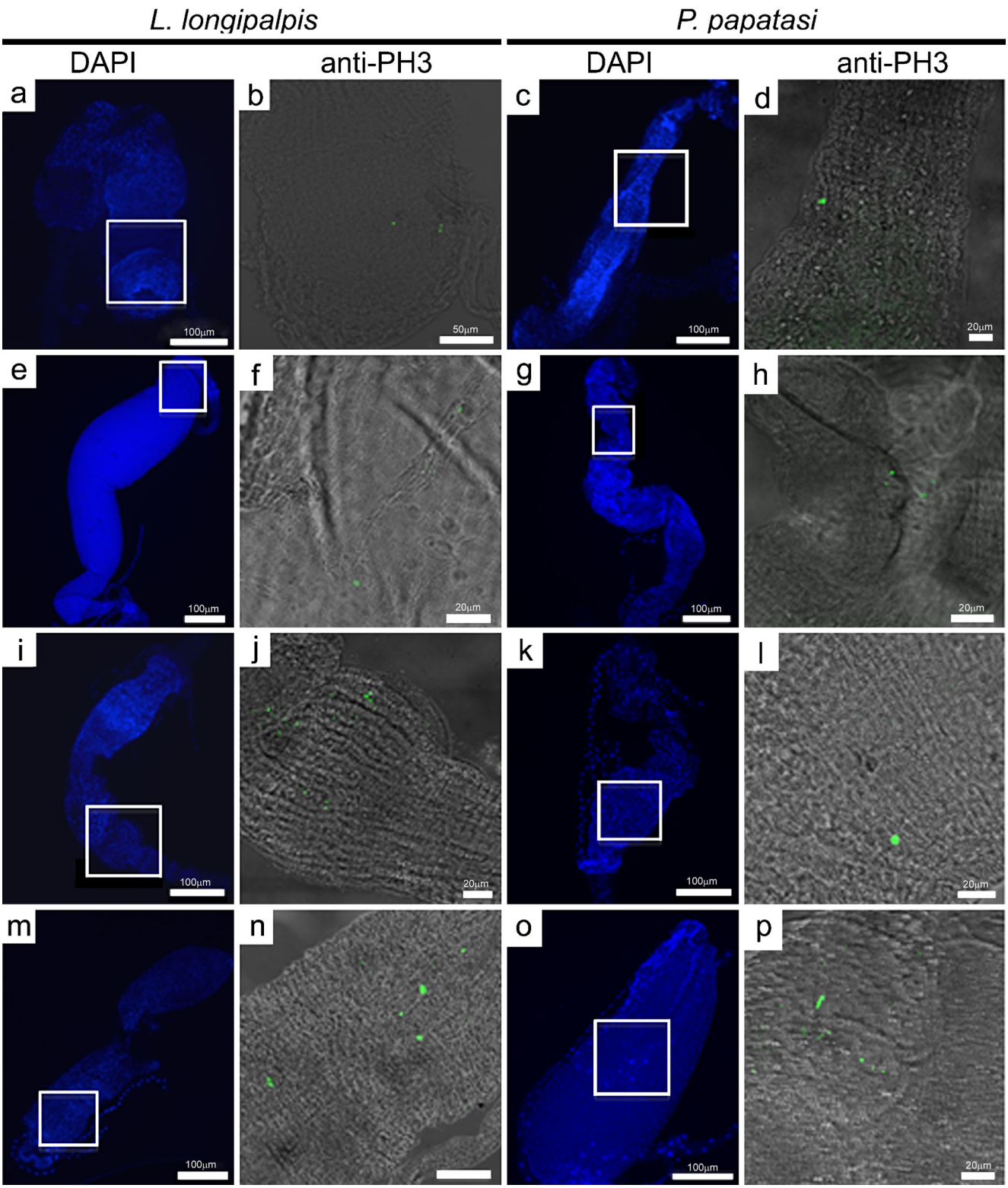

Fig. 6 Marker (*green* fluorescein isothiocyanate [FITC]) of cell proliferation (*PH3* phosphohistone H3) in the midgut of *L. longipalpis* and *P. papatasi*. Samples were observed under the fluorescence microscope, with nuclei stained with DAPI (*blue*). Details of the same samples (*white boxed areas*, *left*) were observed by confocal microscopy (*right*) for the detection of PH3 in L4-5 (**a–d**), pre-pupae (**e–h**), P24 (**i-l**) and P72 (**m–p**)

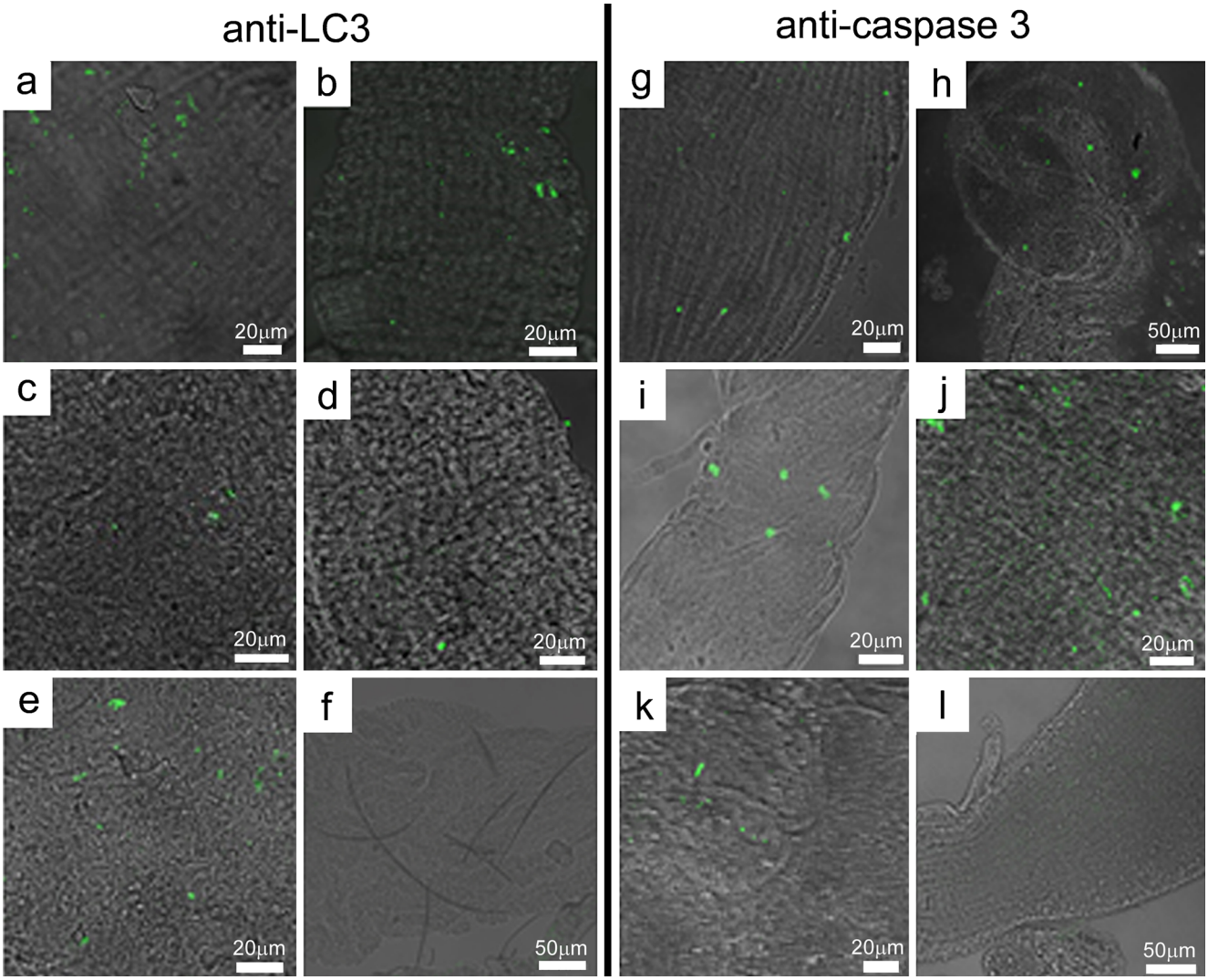

Fig. 7 Markers (*green* FITC) of autophagy (*LC3* LC3A/B [ATG8]) and apoptosis (*caspase 3*) in the midgut of *LLJB* and *PPIS*. *Left* Immunofluorescence in the midgut of *LLJB* (**a**–**c**) and *PPIS* (**d**, **e**) for LC3A/B. Positive staining in *LLJB*: pre-pupa (**a**), P24 (**b**) and P72 (**c**); in *PPIS*: P24 (**d**) and P72 (**e**). Negative control: midgut of P72 of *LLJB* (**f**). *Right* Immunofluorescence for caspase 3 in the midgut of *LLJB* (**g**, **h**) and *PPIS* (**i**–**k**). Positive staining for *LLJB* pre-pupa (**g**) and P72 (**h**) and for *PPIS* pre-pupa (**i**), P24 (**j**) and pP72 (**k**). Negative control: midgut of *LLJB* P24 (**l**)

promoter containing the GAGA motif required for primary response protein binding as described in *B. mori* (Liu et al. 2015) was also observed (Fig. 9). Taken together, these results suggest the presence of a binding site for ecdysone in *ATG1* not only in Lepidoptera, as previously reported (Liu et al. 2015) but also in Diptera. Nevertheless, a conclusive role for ecdysone in the activation of autophagy during metamorphosis in insects in general remains to be established.

Discussion

During metamorphosis, the midgut epithelium undergoes a complete renovation of its differentiated cells allowing the insect to adapt to a new feeding regimen during adulthood. Such cellular renovation of the midgut is crucial as the feeding habits of an insect can change drastically from the larval to the adult stage in holometabolous species. Epithelial remodeling during metamorphosis consists in two major events, namely the degeneration of differentiated cells of the larval epithelium and the proliferation and/or differentiation of stem cells in order to form the new adult midgut epithelium (Parthasarathy and Palli 2007). Previous studies have focused on the remodeling process of the midgut of various holometabolous insects (Neves et al. 2003a, b; Martins et al. 2006; Tettamanti et al. 2007; Franzetti et al. 2012) including some blood-sucking Dipterans (Nishiura et al. 2002; Wu et al. 2006; Parthasarathy and Palli 2007; Ray et al. 2009; Fernandes et al. 2014; 2016). However, little is known of such processes in phlebotomine sand flies whose role as vectors of *Leishmania* have been widely studied.

Table 1 Pro-apoptotic, pro-autophagic and cell division markers at various development stages in sand flies. Qualitative assessment of markers caspase 3 (apoptosis), LC3A/B and ATG6 (autophagy), and phosphohistone H3 (cell proliferation) in the fly midgut during post-embryonic development. Presence (+) or absence (−) of fluorescence signal is indicated for the various developmental stages of the two sand fly species investigated (*nd* not determined, *LLJB L. longipalpis* Jacobina strain, *PPIS P. papatasi* Israeli strain, *L4-5* 5-day-old fourth instar larva, *Pre-pupa* stage during which transition from larval to pupal stages occurs, *P24* pupa at 24 h representing early pupal stage, *P72* pupa at 72 h representing late pupal stage)

Sand fly	Antibody	Developmental stage			
		L4-5	Pre-pupa	P24	P72
LLJB	Caspase 3	-	+	-	+
	Phosphohistone H3	+	+	+	+
	LC3A/B	-	+	+	+
	ATG6	-	nd	+	+
PPIS	Caspase 3	-	+	+	+
	Phosphohistone H3	+	+	+	+
	LC3A/B	-	-	+	+

Several aspects of sand fly physiology resemble that of mosquitoes, including the fact that only females feed on blood. However, sand flies are unique with regards to their ability to transmit *Leishmania* and, interestingly, the *Leishmania* life cycle within the sand fly vector is mostly restricted to the vector midgut, with a crucial developmental step that requires parasite attachment to the gut epithelia (Kamhawi et al. 2004; Ramalho-Ortigão et al. 2010). Here, we investigated the morphological changes in the sand fly midgut during its development from the late larval stage to young adults (females). We also assessed the expression of the autophagy-related genes *ATG1*, *ATG6* and *ATG8* and investigated the expression profiles of *Vein*, a putative EGF. Two sand fly species have been studied in our investigations: *L. longipalpis*, a vector of *Leishmania infantum* and *P. papatasi*, a vector of *Leishmania major*.

The midgut remodeling process during the metamorphosis in mosquitoes includes the programmed cell death of the larval differentiated epithelial cells simultaneously with stem cell proliferation and differentiation to form the adult midgut epithelium (Nishiura et al. 2003; Ray et al. 2009). In sand flies, the pattern of alterations observed in the epithelial cells during midgut metamorphosis shares several features with other holometabolous species (Tettamanti et al. 2007; Franzetti et al. 2012; Romanelli et al. 2016) and specifically with regards to cell regeneration, PH3-positive cells have been reported in mosquitoes (Fernandes et al. 2014).

In lepidopterans, autophagy is activated at the beginning of metamorphosis (Franzetti et al. 2012; Romanelli et al. 2016). Similarly, the degeneration of the larval epithelium in sand flies begins during the fourth instar, with the elimination of differentiated cells and is completed in the pupal stage. During the pre-pupal stage, just after the larval molt, the histolysis of the digestive epithelium becomes more evident by an increase in the number of autophagic vacuoles (some with cellular debris) in the cytoplasm of cells and by the detachment and disposal of these cells toward the midgut lumen, giving space for the expansion of the differentiating cells. In both *LLJB* and *PPIS*, the process occurs in a similar manner from the pre-pupa and is well synchronized for both species as they enter the pupal stage. During the pre-pupal stage, the main difference between the species involves the luminal contents, which are missing in *LLJB*, since the elimination of the larval cells starts later in *LLJB*.

The morphology of midgut epithelial cells dramatically changes during the metamorphosis of insects (Nishiura and Smouse 2000; Neves et al. 2003a, b; Fernandes et al. 2014). In *LLJB* and *PPIS* during metamorphosis, the height of the midgut cells decreases. In pre-pupae, because of the coexistence of old larval digestive cells and cells early in the differentiation process, a disorganized epithelium is seen. A shorter cell height in P24 is possibly attributable to the prevalence of many small cells undergoing differentiation. In the RE adults, newly differentiated cells are tall and elongated, with re-established microvilli, and the mean height of the midgut epithelium is greater than that seen in the pupae, probably because of the elimination of the luminal contents, which permits cell expansion toward the midgut lumen.

Cells under differentiation were seen in the pre-pupal and pupal stages of both sand flies. The morphological characteristics of cells in differentiation seen here have also been reported during midgut metamorphosis in other insects (Neves et al. 2003a, b; Rost-Roszkowska et al. 2010; Fernandes et al. 2014). During differentiation, the regenerative cells lengthen toward the lumen, the nucleus becomes more prominent, and organelles become more conspicuous. The accumulation of mitochondria in the apical supranuclear region of cells is an important signal of cell differentiation and may help the cell to reach the lumen of the midgut (Rost-Roszkowska et al. 2010). As the cell differentiation process advances, short and folded microvilli are seen at the apex of these cells.

Whereas many midgut cells are still undergoing differentiation, undifferentiated stem cells form a group based on the epithelium of P72 *LLJB*. These stem cells remain undifferentiated in the pupa and will be presumably responsible for originating other nests of stem cells during pupation (Neves et al. 2003a, b). Stem cells are present in the midgut of insects not only during post-embryonic development. In adult *Culex quinquefasciatus*, for example, the replacement and/or renewal of midgut epithelial cells after feeding on blood takes place by the differentiation of pre-existing stem cells (Okuda et al. 2007).

Cell proliferation and cell death have been shown to be critical in defining the overall size of the insect midgut, as the balance between cell degeneration and regeneration establish

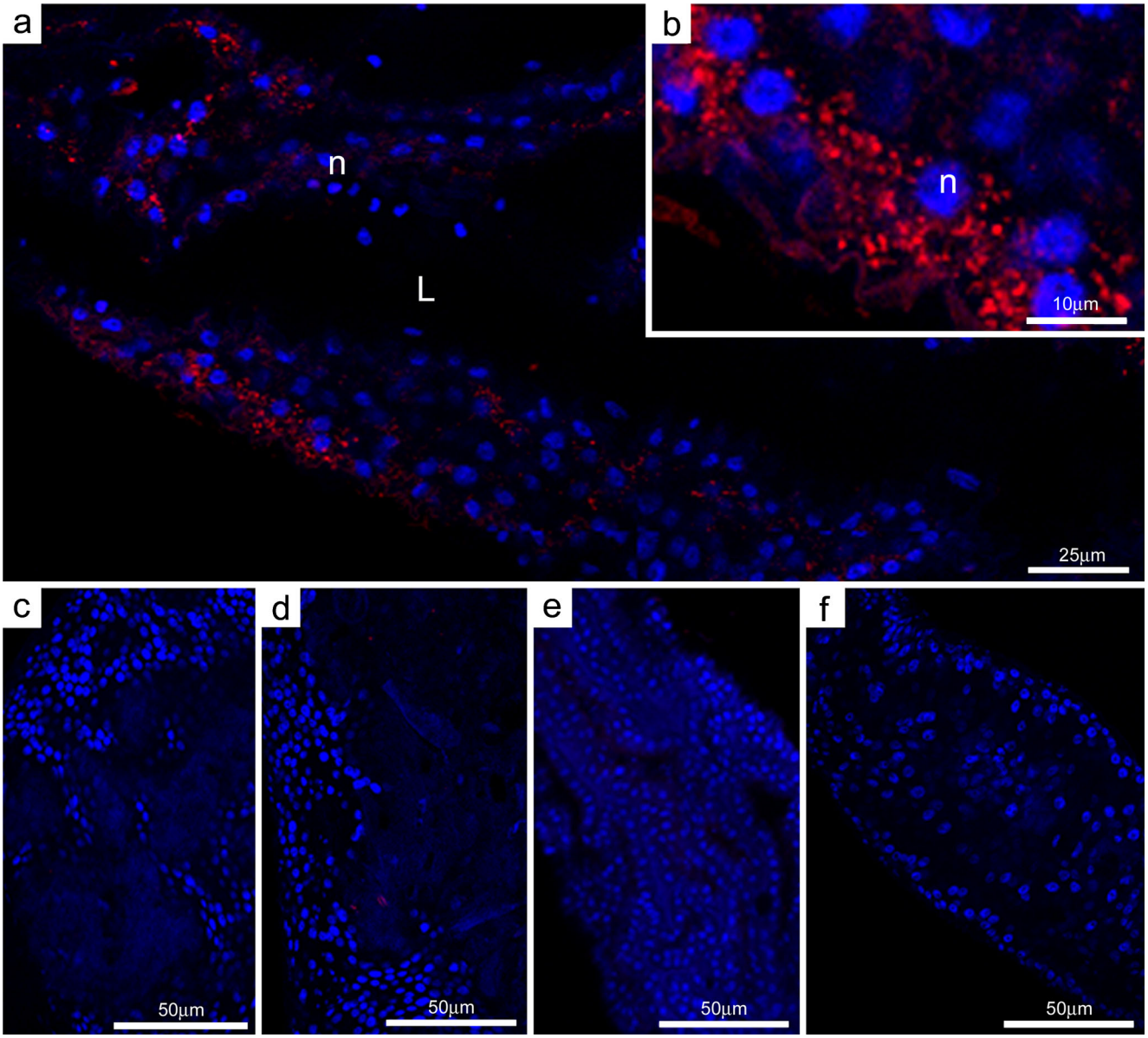

Fig. 8 Expression of the autophagy-related protein ATG6 in *LLJB* midgut. **a** Confocal images showing the anterior midgut of newly formed pupae. Cell nuclei (*n*) are stained *blue* (DAPI) and the positive marker for ATG6 is in *red* (*L* lumen). **b** Detail of the red staining for ATG6 in the cytoplasmic compartments of epithelial cells (*n* nucleus). **c–e** Images showing the anterior midgut of L3, L4 and adult, respectively, with little to no signal for ATG6. **f** Negative control: midgut of *LLJB* L3

the number of cells during midgut development (Sonakowska et al. 2016). The presence of PH3-positive (i.e., mitotic) cells in the midgut of both *LLJB* and *PPIS* suggests that, even during metamorphosis when the sand fly midgut undergoes significant changes, stem cell division still takes place and might contribute to midgut growth. The proliferation of stem cells has been reported in mosquitoes as being important to the process of the renewal of the midgut epithelium during metamorphosis (Nishiura and Smouse 2000; Nishiura et al. 2005; Fernandes et al. 2014). Further, as described for *A. aegypti* (Nishiura et al. 2003; Fernandes et al. 2014), the proliferation of stem cells in sand flies begins shortly after the last larval molt (L3-L4) and continues in the pupa.

Apoptosis and autophagy have been reported to occur simultaneously during metamorphosis in the midgut epithelium in *D. melanogaster*, with morphological features of autophagic cell death and components of apoptosis (Lee et al. 2002). However, the remodeling of fruit fly midgut is controversial. According to Denton et al. (2009), autophagy and not apoptosis, is critical to the process of cell death in the gut of *D. melanogaster* during metamorphosis. In this case, the pathway of apoptotic caspase activation is not required for the cell

Fig. 9 Predicted *ATG1* promoter sequence in *LLJB*: the 941 bp upstream of the predicted Met (ATG start codon indicated by *arrow* and *box*) containing three putative half-sites for ecdysone receptor protein binding (*black boxes*) and a cluster of four potential GAGA sequences for primary response gene binding (*underlined* and *asterisks*)

death process in the midgut during metamorphosis in this insect.

The death of the epithelial cells during the metamorphosis of the midgut of *A. aegypti* has been described as a process of programmed cell death dependent on caspases (Parthasarathy and Palli 2007). The presence of autophagic vacuoles in the epithelial cells in *LLJB* and *PPIS*, especially in the larval-pupal transition, combined with our analysis of the profiles of expression of *ATG1*, *ATG6* and *ATG8*, strongly suggests that, in sand flies, the degenerative process of the digestive epithelium occurs by autophagy, leading to the death of larval digestive cells. Additionally, the presence of positive markers for ATG6, LC-3/ATG8 and caspase-3 in the pre-pupal and/or pupal stage in sand flies suggests that processes of both autophagy and apoptosis occur during the degeneration of the epithelium in the larval-pupal transition. This is similar to the situation in *B. mori*, in which autophagy starts in the fifth instar larvae and amplifies within pre-pupae, whereas apoptosis occurs from the pre-pupal stage (Franzetti et al. 2012). Moreover, the presence of the LC3 form of ATG8 implies the lipidation (phosphotidylethanolamine) of the protein suggestive of mature autophagosomes preparing to fuse with lysosomes (Nath et al. 2014). In this case, apoptosis participates in the elimination of the larval differentiated midgut cells, whereas autophagy assists in the recycling of nutrients during pupation when the insect does not feed. Thus, we can reasonably propose that the histolysis of the larval digestive cells in sand flies occurs by autophagy and cell death, as is the case in other holometablous insects such as *A. aegypti* and *B. mori* (Fernandes et al. 2014; Romanelli et al. 2016). In addition, we observed anti-ATG6 staining in the epithelial cells of the pupa, consistent with its role in the removal of the larval gut or as a pro-apoptotic response (Franzetti et al. 2012).

We also detected an up-regulation of the putative EGF *Vein* in L4 and pupa. We previously described the likely role of Vein following the infection of *L. longipalpis* larvae with *Bacillus subtilis* and *Pantoea agglomerans* (Heerman et al. 2015). Vein probably provides the signals necessary for the development of

adult sand fly tissues within the puparium, as suggested from studies in *Drosophila* (Jiang and Edgar 2009; Biteau and Jasper 2011). Although the upregulation of *Vein* in both L4 and pupae may be associated with the beginning of adult tissue formation in the sand fly pupa, we have yet to determine whether it is localized to midgut stem cells.

An understanding of the link between ecdysone signaling and autophagy during insect metamorphosis is of physiological relevance. Whereas a recent biochemical study (Liu et al. 2015) shed light on this mechanism within Lepidoptera, nothing is known about this phenomenon within Diptera. In *LLJB*, we found genomic evidence to suggest that this phenomenon exists across multiple orders of holometabolous insects. Although we described the presence of a canonical ecdysone responsive element (Cherbas et al. 1991) in the promoter of *ATG1* in *LLJB*, we have yet to identify a similar sequence in the genome of *PPIS*; issues related to the current *PPIS* genome scaffolding prevented us from doing so at this point. Furthermore, we were unable to identify binding sites for E93 in sand flies, as previously described for *B. mori* (Liu et al. 2015). The determination of the way that *ATG1* promoters in sand flies and potentially other hematophagous Dipterans, are associated with the control of the onset of metamorphosis in these insects should provide crucial details about their development and possibly offer novel methods for their control.

Acknowledgements We are grateful to the Núcleo de Microscopia e Microanálise (NMM) Universidade Federal de Vicosa (UFV) for the use of their microscopy facility, including transmission and confocal microscopes, and for technical assistance. To the Molecular Systematics Laboratory, Department of Animal Biology, UFV, for the use of their epifluorescence microscope. This study was partially funded with a grant from the Coordenação de Aperfeiçoamento de Pessoal de Nível Superior (CAPES/PVE 88881.030429/2013-01).

References

Andrade-Coêlho CA, Santos-Mallet J, Souza NA, Lins U, Meirelles MN, Rangel EF (2001) Ultrastructural features of the midgut epithelium of females *Lutzomyia intermedia* (Lutz & Neiva, 1912) (Diptera: Psychodidae: Phlebotominae). Mem Inst Oswaldo Cruz 96:1141–1151

Berry DL, Baehrecke EH (2007) Growth arrest and autophagy are required for salivary gland cell degradation in *Drosophila*. Cell 131:1137–1148

Biteau B, Jasper H (2011) EGF signaling regulates the proliferation of intestinal stem cells in *Drosophila*. Development 138:1045–1055

Buchon N, Broderick NA, Kuraishi T, Lemaitre B (2010) *Drosophila* EGFR pathway coordinates stem cell proliferation and gut remodeling following infection. BMC Biol 8:152

Cherbas L, Lee K, Cherbas P (1991) Identification of ecdysone response elements by analysis of the *Drosophila* Eip28/29 gene. Genes Dev 5:120–131

Coutinho-Abreu IV, Sharma NK, Robles-Murguia M, Ramalho-Ortigão M (2010) Targeting the midgut secreted PpChit1 reduces *Leishmania major* development in its natural vector, the sand fly *Phlebotomus papatasi*. PLoS Negl Trop Dis 4:e901

Denton D, Shravage B, Simin R, Mills K, Berry DL, Baehrecke EH, Kumar S (2009) Autophagy, not apoptosis, is essential for midgut cell death in *Drosophila*. Curr Biol 19:1741174–6

Denton D, Chang TK, Nicolson S, Shravage B, Simin R, Baehrecke EH, Kumar S (2012) Relationship between growth arrest and autophagy in midgut programmed cell death in *Drosophila*. Cell Death Differ 19:1299–1307

Fernandes KM, Neves CA, Serrão JE, Martins GF (2014) *Aedes aegypti* midgut remodeling during metamorphosis. Parasitol Int 63:506–512

Fernandes KM, Magalhães-Júnior MJ, Baracat-Pereira MC, Martins GF (2016) Proteomic analysis of *Aedes aegypti* midgut during post-embryonic development and of the female mosquitoes fed different diets. Parasitol Int 65:668–676

Franzetti E, Huang ZJ, Shi YX, Xie K, Deng XJ, Li JP, Li QR, Yang W, Zeng W, Casartelli M, Deng H, Cappellozza S, Grimaldi A, Xia Q, Tettamanti G, Cao Y, Feng Q (2012) Autophagy precedes apoptosis during the remodeling of silkworm larval midgut. Apoptosis 17:305–324

Gemetchu T (1974) The morphology and fine structure of the midgut and peritrophic membrane of the adult female, *Phlebotomus longipes* Parrot and Martin (Diptera: Psychodidae). Ann Trop Med Parasitol 68:111–128

Hakim RS, Baldwin K, Smagghe G (2010) Regulation of midgut growth, development, and metamorphosis. Annu Rev Entomol 55:593–608

Heerman M, Weng JL, Hurwitz I, Durvasula R, Ramalho-Ortigão M (2015) Bacterial infection and immune responses in *Lutzomyia longipalpis* sand fly larvae midgut. PLoS Neg Trop Dis 9:e0003923

Jiang H, Edgar BA (2009) EGFR signaling regulates the proliferation of *Drosophila* adult midgut progenitors. Development 136:483–493

Kamhawi S, Ramalho-Ortigao M, Pham VM, Kumar S, Lawyer PG, Turco SJ, Barillas-Mury C, Sacks DL, Valenzuela JG, Valenzuela JG (2004) A role for insect galectins in parasite survival. Cell 119:329–341

Killick-Kendrick R (1999) The biology and control of phlebotomine sandflies. Clin Dermatol 17:279–289

Lainson R, Rangel EF (2005) *Lutzomyia longipalpis* and the eco-epidemiology of American visceral leishmaniasis, with particular reference to Brazil: a review. Mem Inst Oswaldo Cruz 100:811–827

Lee CY, Cooksey BA, Baehrecke EH (2002) Steroid regulation of midgut cell death during *Drosophila* development. Dev Biol 250:101–111

Liu X, Dai F, Guo E, Li K, Ma L, Tian L, Cao Y, Zhang G, Palli SR, Li S (2015) 20-Hydroxyecdysone (20E) primary response gene E93 modulates 20E signaling to promote *Bombyx* larval-pupal metamorphosis. J Biol Chem 290:27370–27383

Malta J, Martins GF, Weng JL, Fernandes KM, Munford ML, Ramalho-Ortigão M (2016) Effects of specific antisera targeting peritrophic matrix-associated proteins in the sand fly vector *Phlebotomus papatasi*. Acta Trop 159:161–169

Martins GF, Neves CA, Campos LAO, Serrão JE (2006) The regenerative cells during the metamorphosis in the midgut of bees. Micron 37:161–168

McPhee CK, Balgley BM, Nelson C, Hill JH, Batlevi Y, Fang X, Baehrecke EH (2013) Identification of factors that function in *Drosophila* salivary gland cell death during development using proteomics. Cell Death Differ 20:218–225

Nath S, Dancourt J, Shteyn V, Puente G, Fong MW, Nag S, Bewersdorf J, Yamamoto A, Antonny B, Melia JT (2014) Lipidation of the LC3/GABARAP family of autophagy proteins relies upon a membrane curvature-sensing domain in Atg3. Nat Cell Biol 16:415–424

Neves CA, Gitirana LB, Serrão JE (2003a) Ultrastructural study of the metamorphosis in the midgut of *Melipona quadrifasciata anthidioides* (Apidae, Meliponini) worker. Sociobiology 41:443–459

Neves CA, Gitirana LB, Serrão JE (2003b) Ultrastructure of the midgut endocrine cells in *Melipona quadrifasciata anthidioides* (Hymenoptera, Apidae). Braz J Biol 63:683–690

Nishiura JT, Smouse D (2000) Nuclear and cytoplasmic changes in the *Culex pipiens* (Diptera: Culicidae) alimentary canal during metamorphosis and their relationship to programmed cell death. Ann Entomol Soc Am 93:282–290

Nishiura JT, Ho P, Ray K (2003) Methoprene interferes with mosquito midgut remodeling during metamorphosis. J Med Entomol 40:498–507

Nishiura JT, Ray K, Murray J (2005) Expression of nuclear receptor-transcription factor genes during *Aedes aegypti* midgut metamorphosis and the effect of methoprene on expression. Insect Biochem Mol Biol 35:561–573

Okuda K, Almeida F de, Mortara RA, Krieger H, Marinotti O, Bijovsky AT (2007) Cell death and regeneration in the midgut of the mosquito, *Culex quinquefasciatus*. J Insect Physiol 53:1307–1315

Parthasarathy R, Palli SR (2007) Stage- and cell-specific expression of ecdysone receptors and ecdysone-induced transcription factors during midgut remodeling in the yellow fever mosquito, *Aedes aegypti*. J Insect Physiol 53:216–229

Ramalho-Ortigão M, Saraiva EM, Traub-Csekö YM (2010) Sand fly-*Leishmania* interactions: long relationships are not necessarily easy. Open Parasitol J 1:195–204

Rangel EF, Lainson R (2003) Ecologia das leishmanioses. In: Rangel EF, Lainson R (eds) Flebotomíneos do Brasil. FIOCRUZ, Rio de Janeiro, pp 291–311

Ray K, Mercedes M, Chan D, Choi CY, Nishiura JT (2009) Growth and differentiation of the larval mosquito midgut. J Insect Sci 9:1–13

Romanelli D, Casartelli M, Cappellozza S, Eguileor M de, Tettamanti G (2016) Roles and regulation of autophagy and apoptosis in the remodeling of the lepidopteran midgut epithelium during metamorphosis. Sci Rep 6:32939

Rost-Roszkowska MM, Vilimova J, Chajec L (2010) Fine structure of the midgut epithelium in *Atelura formicaria* (Hexapoda, Zygentoma, Ateluridae), with special reference to its regeneration and degeneration. Zool Stud 49:10–18

Rudin W, Hecker H (1982) Functional morphology of the midgut of a sandfly as compared to other hematophagous nematocera. Tissue Cell 14:751–758

Rusten TE, Lindmo K, Juhasz G, Sass M, Seglen PO, Brech A, Stenmark H (2004) Programmed autophagy in the *Drosophila* fat body is induced by ecdysone through regulation of the PI3K pathway. Dev Cell 7:179–192

Sádlová J, Volf P (2009) Peritrophic matrix of *Phlebotomus duboscqi* and its kinetics during *Leishmania major* development. Cell Tissue Res 337:313–325

Schmittgen TD, Livak KJ (2008) Analyzing real-time PCR data by the comparative CT method. Nat Protocols 3:1101–1108

Secundino NFC, Eger-Mangrich I, Braga EM, Santoro MM, Pimenta PFP (2005) *Lutzomyia longipalpis* peritrophic matrix: formation, structure, and chemical composition. J Med Entomol 42:928–938

Sherlock ÍA (2003) A importância dos flebotomíneos. In: Rangel EF, Lainson R (eds) Flebotomíneos do Brasil. FIOCRUZ, Rio de Janeiro, pp 337–351

Siegmund T, Lehmann M (2002)The *Drosophila* Pipsqueak protein defines a new family of helix-turn-helix DNA-binding proteins.Dev Genes Evol 212:152–157

Sonakowska L, Włodarczyk A, Wilczek G, Wilczek P, Student S, Rost-Roszkowska M (2016) Cell death in the epithelia of the intestine and hepatopancreas in *Neocaridina heteropoda* (Crustacea, Malacostraca). PLoS ONE 11:e0147582

Tettamanti G, Grimaldi A, Casartelli M, Ambrosetti E, Ponti B, Congiu T, Ferrarese R, Rivas-Pena ML, Pennacchio F, Eguileor M de (2007) Programmed cell death and stem cell differentiation are responsible for midgut replacement in *Heliothis virescens* during pre-pupal instar. Cell Tissue Res 330:345–359

Tian L, Ma L, Guo E, Deng X, Ma S, Xia Q, Cao Y, Li S (2013) 20-Hydroxyecdysone upregulates Atg genes to induce autophagy in the *Bombyx* fat body. Autophagy 9:1172–1187

Vale VF do, Pereira MH, Gontijo NF (2007) Midgut pH profile and protein digestion in the larvae of *Lutzomyia longipalpis* (Diptera: Psychodidae). J Insect Physiol 53:1151–1159

Wigglesworth VB (1972) The principles of insect physiology. Chapman and Hall, London

Wu Y, Parthasarathy R, Bai H, Palli SR (2006) Mechanisms of midgut remodeling: juvenile hormone analog methoprene blocks midgut metamorphosis by modulating ecdysone action. Mech Dev 123:530–547